INTERNATIONAL JOURNAL OF ADVANCE RESEARCH, IDEAS AND INNOVATIONS IN TECHNOLOGY

**ISSN: 2454-132X**
**Impact factor: 4.295**
***(Volume 5, Issue 6)***
Available online at: www.ijariit.com

# Study of ZnO Nanoparticles for Gas Sensing Application

*Mriganko Bastav Chakravertty*
*bastavedmundz@gmail.com*
*University of Delhi, New Delhi, Delhi*

## ABSTRACT

***This report presents a brief discussion on the importance of ZnO nanomaterial in gas sensing application. Recent developments on ZnO-based gas sensors have been reviewed. The primary work in this report involves the study of the Raman spectrum of a ZnO wurtzite sample. Using the group theoretical background, the various vibrational modes of the ZnO wurtzite have been studied at length. Finally, the defect properties of ZnO wurtzite, mainly the oxygen vacancy defect which plays an important role in gas sensing application, have been investigated.***

***Keywords***— *Gas sensors, Phonon, Wurtzite, Nanomaterial*

## 1. INTRODUCTION

Metal oxide semiconductors are extensively used for gas sensing application. ZnO has potential applications in electronics, photonics, acoustics etc. ZnO based gas sensors are important because ZnO is sensitive towards various adsorbed gases and has high chemical stability. ZnO based gas sensors are use full for the detection of gases such as $NO_2$, $H_2S$, Ethanol vapor etc. The sensing property of the ZnO is attributed to its defect properties. Due to the presence of intrinsic defect such as oxygen vacancy and zinc interstitials even undoped ZnO exhibits an *n-type* conductivity.

### 1.1 What is a Nanomaterial?

Materials with at least one of the dimensions measuring less than 100 nm are known as nanomaterial [1]. Alternatively, nanomaterial is defined as those materials whose characteristic length scale ranges within 100 nm. Based on the confinement of the number of dimensions to nano-scale, nanomaterial can be divided into four groups viz. Zero-Dimensional (0D), One-Dimensional (1D), Two-Dimensional (2D), Three-Dimensional (3D). The properties of the bulk-materials are mostly retained till the reduction of their dimensions to the micrometer range. But materials in the nanometer scale may show remarkably new properties. Important examples of 1D nanostructure include carbon nanotubes, quantum wires, and conducting polymers. Examples of zero dimensional systems are semiconductor nano-crystal, metal Nanoparticles (NPs), and lithographically patterned quantum dots [2].

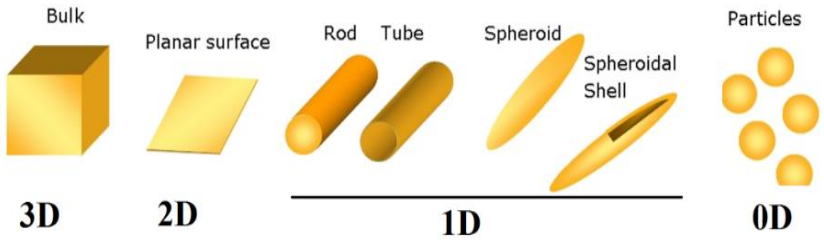


**Fig. 1: Nanostructures in different dimensions.**

### 1.2 Need of nanomaterial in gas sensing application

As mentioned earlier the properties of nanomaterial are different from the bulk material. Two factors which are responsible for this change in the properties are:

**Increase in surface to volume ratio:** This can be explained with the example of a cube. When a cube of side, say 1cm is divided into eight small cubes of side 0.5cm each than the sum of the areas of the 8 small cubes is much larger than the volume of the large cube. The surface to volume ratio comes out to be 12.

 

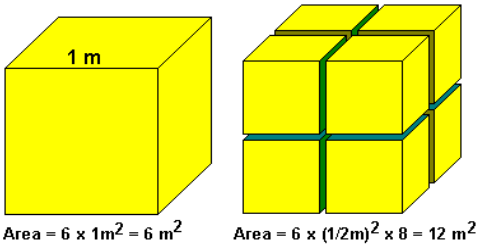


**Fig. 2: Surface to volume ratio increase of a cube**

**Quantum confinement:** An electron in a 3 D box of side $L_X$, $L_Y$ and $L_z$ is a system that is well studied to understand the behavior of the free electron and to finally find the energy eigenvalues. When the electron is free in all dimensions, we mean that the de-Broglie wavelength of the electron $\chi << L_x, L_y$, and $L_z$ [3]. Under such conditions imposed on the electron, when the Schrödinger's equation is solved it yields the electron energy to be discrete. However, if the dimensions of the box are large it essentially gives a continuous energy level. We now assume that we make the box small in size such that the above condition is reversed i.e. now we have $\chi \geq Lx, Ly$, and $L_z$. Since $L_x, L_y, L_z$ are now relatively small the energy of the electron $E_{nx, ny, nz}$ is discrete. Electron movement will be confined in all three directions, exhibiting energy quantization in all three dimensions and the electron will not be free in any of the dimensions. This makes for an effectively zero-dimensional system called a quantum dot. Thus when the size of a particle is very small the discreteness in energy is very prevalent. In the realm where the dimension of the particle is comparable with the de-Broglie wavelength confinement is imposed to the randomly moving electron and the motion is restricted to specific energy levels. Decrease in confining dimensions ultimately increases or widens up the band gap. Since band gap and wavelength is inversely proportional the wavelength decreases. Quantum confinement is defined as the change in the electronic and optical properties of a material when the material sampled is of sufficiently small size-typically 10nm or less. Increase in surface area increases the receptor action whereas due to quantum confinement the changed electrical and optical properties enhance the transducer action. The following are some reviews on ZnO nanostructure and its sensing property.

### 1.3 ZnO nanostructure and its gas sensing properties, a review

Kumar *et al.* [4] reviewed some aspects of the structural properties of a ZnO nanostructure, Wurtzite, and demonstrated its gas sensing property. Target material is identified by the receptor mechanism. The chemical stimulus is transformed into an electric pulse by a transducer. A major role in gas detection capability of a material is played by its structural form. Out of many possible structures, wurtzite is most favored form of ZnO. The crystalline property of ZnO is given in Table .1. The HCP structure is shown in the following figures (3).

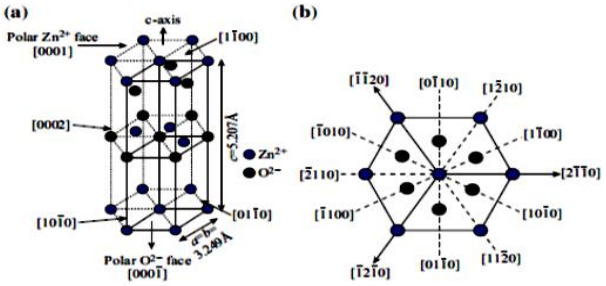


**Fig. 3: (a) Unit cell of ZnO wurtzite structure (b) Hexagonal base of the unit cell**

**Table 1: Properties of ZnO, Wurtzite structure**

| | |
|---|---|
| Lattice parameters | a =3.249Å, c=5.207Å |
| Structure | Interconnected HCP sub-lattices in hexagonal lattice of $Zn^{2+}$ and $O^{2-}$. |
| Space Group | P63mc |
| Hybridization | $SP^3$ |
| Symmetry | Centrosymmetric (Lacks inversion symmetry) |
| Electrical Properties | Piezoelectric, Pyroelectric |

The ionic nature of the ZnO material results in polarity of the sample. This polarity is exhibited in a periodic manner in the c-axis. The surfaces [0001] and [000$\bar{1}$] faces of ZnO are terminated by Zn and O respectively. The units are repeated in a perpendicular direction w.r.t. to c-axis and hence a dipole moment along that direction comes into play. Polar surfaces generally exhibit such property and due to bulk-truncation such structures lack stability. However, these surfaces are stable. These surfaces are stabilized by extra ions or cations or electrons. This indicates that there is a sufficient mechanism accounting for the stability. These stabilization mechanisms may also influence the gas sensing properties of ZnO. ZnO is an *n*-type semiconductor with electrons as current carriers. The adsorption of molecular and atomic oxygen on the surface of ZnO NPs creates an electron-depleted space-charge layer which is regarded as an important characteristic of the receptor function.

Han et al. [5] demonstrated that the gas sensing performance of ZnO is affected by its crystal defects. For high level of oxygen vacancies there exists a higher gas response of ZnO. The second function, viz. transducer function, depends upon interactions of analyte gas and the ZnO nanoparticles. Two types of interactions are considered to be important which may be either grain-boundary or neck interactions. In the grain-boundary contacts, the movement of the electrons takes place for each boundary across the surface potential barrier. Hence, the barrier height is changed and the electrical resistance of the sensor material is also changed. But the

 

resistance and the gas response are not a function of the particle size. For the neck contacts, the electron is transferred through channels due to the space-charge region. This channel width depends on the neck size and thus the resistance changes with the channel width. When the particle size decreases, the sensor material loses the mobile charge carriers. The gas sensing property can also be enhanced by decreasing the particle size and increasing the surface to volume ratio. ZnO NPs having size of few nm contains high density of grain boundary and offers higher interactions with gases such as $NO_2$.

**1.4 Role of oxygen vacancy defect in the gas sensing property of ZnO.**

Oxygen vacancies and defects in lattice provide adsorption sites for oxygen and test gases. Gas detection process originates from the interaction of the adsorbed oxygen atoms present in gases and the gas itself. Thus, the response is directly proportional to the defect density. At low temperature $O_2^-$ is chemisorbed whereas at high temperature $O^-$ and $O^{2-}$ are chemisorbed and $O^{2-}$ disappears. The oxygen ion portion has the ability to extract the conduction electron from ZnO and lower the conductance. The ion species such as $O^{2-}$, $2O^-$ and $O^-$ which are reactive and adsorbed on ZnO surface with the increase in temperature. Gas sensing property of defect controlled ZnO-nanowire was studied by Ahn et al [5]. The following equilibrium exists between oxygen gas and adsorbed oxygen.

$$O_2(gas) \leftrightarrow O_2(adsorbed)$$

$$O_2(adsorbed) + e^- \leftrightarrow O_2^-(adsorbed)$$

$$O_2(adsorbed) + 2e^- \leftrightarrow 2O^-(adsorbed)$$

$$O^-(adsorbed) + e \leftrightarrow O_2^-(adsorbed)$$

The reaction involved in the detection of $NO_2$ and $H_2S$ gases is shown below.

**1.4.1 Detection of $NO_2$:** ZnO nanostructures for $NO_2$ gas sensing was studied by Kumar *et al* [4]. $NO_2$ is an oxidizing gas. These molecules readily get adsorbed onto the surface of the thin film (ZnO) by directly extracting electrons from the conduction band or they can even interact with the chemisorbed oxygen on the surface. The reactions involved are as follows:

$$NO_2(gas) + e^- \rightarrow NO_2^-(adsorbed)$$

$$NO_2(gas) + O_2^-(adsorbed) + 2e^- \rightarrow NO_2^-(adsorbed) + 2O^-(adsorbed)$$

The equations reveal that the electrons are consumed in the reactions which results in the decrease in the conductivity of the ZnO thin film. The concentration of the free electrons is reduced. It is also seen that the adsorbed $O_2^-$ ions plays an important role in the metal-oxide gas sensing. These ions tend to direct the $NO^{2-}$ ions in extracting the electron from the ZnO thin film.

**1.4.2 Detection of $H_2S$:** $H_2S$ gas decreases the resistance of the ZnO film by releasing electron in conduction band. This release is indeed brought about by the chemisorbed oxygen.

$$H_2S(gas) + O_2^-(adsorbed) \leftrightarrow H_2S(adsorbed) + O_2(gas) + e^-$$

$$2H_2S(adsorbed) + O_2^-(adsorbed) \leftrightarrow 2SO_2 + 2H_2O + 3e^-$$

This reaction shows that there is an increase in the number of electron (the reaction infuses electrons into the sensing layer) thereby decreasing the sensor resistance. In addition to the surface reaction with $O_2^-$, chemical conversion of ZnO with $H_2S$ is another possible reaction mechanism affecting the conductivity of the ZnO sensor. The chemical conversion of the gas sensing material through direct reaction with the target gas is known to be an important mechanism that changes the conductivity and produces high sensitivity in several sensing material of metal oxide. The sensitivity of a gas sensor is defined as the percentage change in the resistivity of the sensing material on exposure to the target gas.

$$S(\%) = \frac{Rg - Ra}{Ra} \times 100$$

Where $Rg$ and $Ra$ are the resistances of the sensing material in air and in presence of target gas respectively.

## 2. THEORETICAL BACKGROUND

**2.1 Raman scattering in solids**

Light can be scattered both elastically and in-elastically by a solid. Raman scattering is an inelastic scattering of light. An atom or a molecule placed in an electric field experiences an induced dipole moment and thus the molecule is polarized. Various scattering processes can take place in a solid. The oscillating electric field induces vibration in the atoms in the lattice, yielding a photon. Thus, a photon-phonon interaction can take place giving rise to the stoke or the anti-stokes scattering depending on whether a photon is created or annihilated respectively during the process.

 

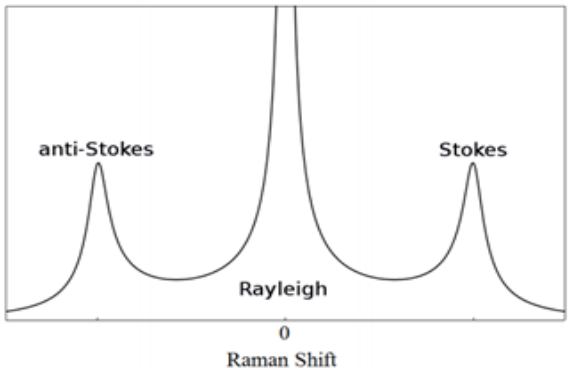


**Fig. 4: Raman Spectrum of a sample consists of stokes and anti-stokes lines both symmetrically located about the Rayleigh scattered component of the laser light.**

Raman spectrum of a sample can reveal important information about the vibrational properties that can be linked with the defects and oxygen vacancies in the crystal. Study of the Raman spectrum requires an understanding of the vibrational modes of a crystal and the symmetry associated with its Bravais lattice.

**2.2 Vibrations in a crystal**

Sound waves or elastic waves in a crystal are said to be composed of phonons. Whenever there is a wave generated due to the influence of thermal energy or thermal gradient waves are generated in a crystal which propagates through the lattice. Lattice vibrations are quantized and the quantum of energy associated with a particular mode of vibration is known as phonon. The energy associated with vibration of frequency v is given by. For a monoatomic linear chain of atoms in a one-dimensional lattice the angular frequency depends on the wave vector k by a Sine function multiplied by a constant. The dispersion relation in a diatomic linear chain yields two different branches, the acoustic modes and the optical modes.

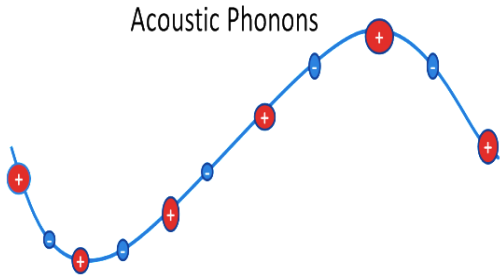


**Fig. 5: Acoustical mode in a diatomic linear lattice**

Physically, a lattice phonon does not carry any momentum, but it interacts with other particles and fields as if it has a momentum given by $= \frac{hk}{2\pi}$. This quantity is sometimes called the crystal momentum. In three dimensions, there exists a generalization that for $p$ atoms per unit cell of a crystal, there are 3 acoustic branches and 3$p$-3 optical branches. Furthermore, there can be Longitudinal Acoustic (LA), Transverse Acoustic (TA), Longitudinal Optical (LO) and Transverse Optical (TO) modes depending on direction of vibration of the atoms with respect to the direction of propagation of the waves in the lattice. These phonons can be treated as quasi particle and can take part in scattering processes. Whenever an electromagnetic wave travels through a crystal the electric field vector induces vibrations in the charged species of the crystal which produces phonons. Thus, it gives rise to photon-phonon interaction and in these interactions wave vector is always conserved. In case of inelastic scattering of photons, the momentum of the incident photon change.

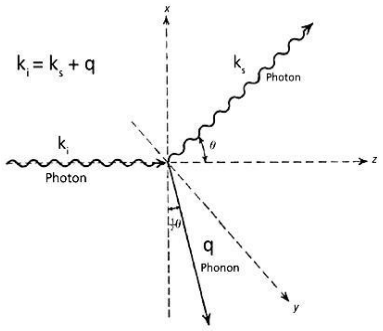


**Fig. 6: Inelastic scattering of photon of wave vector $k_i$ to produce scattered photon of wave vector $k_s$ with the emission of a phonon of wave vector q.**

Thus, the wave vector conservation law reads,

$$k_i = k_s + q,$$

 

Certain lattice vibrational modes can be active as fundamentals in Raman and Infrared studies [6]. For an ionic crystal, the oscillating electric field component of the electromagnetic radiation induces dipole moment of vibrational transition $\mu_y$ when the wave travels in the *x* direction and a dipole moment of vibrational transition $\mu_x$ when the wave travels in the *y* direction. Some vibrational modes are localized at specific points in the crystal lattice and can be described by the motion of the atoms around that point. Such modes are called the local mode vibrations. Whereas, in an extended lattice, the vibrations are collective and can be described by normal mode vibration. To elucidate the various modes of vibration in a lattice it is important to study the symmetry properties related to the crystal structure. The irreducible representation of the various modes of vibration in a crystal can be elucidated from the character table of the point group related to the symmetry of the particular crystal. Hence it is necessary to have a clear understanding of the symmetry of a crystal. The following section provides a brief discussion on symmetry properties of crystal and its group theoretic implications.

## 3. SYMMETRY PROPERTIES OF A CRYSTAL AND GROUP THEORY

A symmetry operation is defined as operation which transforms the crystal into itself i.e. the crystal remains invariant under a symmetry operation. A three-dimensional crystal lattice can have the symmetry elements viz. Identity (E), Proper axis of rotation ($C_n$), Plane of symmetry ($\sigma$), Improper axis of rotation or rotation-reflection ($S_n$) and Inversion center or center of symmetry(i). Depending on the geometrical shape the unit cell the crystal lattice may have different operations transforming the crystal to itself. All such operations constitute the symmetry operations of the crystal. These symmetry operations form a mathematical group. A translation group is given by {E|**T**} where E is the identity element and **T** is the translation operation [7]. A point group has operation given by {$\alpha$|0} where $\alpha$ is a symmetry operation at a point that leaves the system invariant with no translation. Whereas a space group operation has combined point operations and translations that leaves the system invariant. The symmetry operations of a point group include rotation about an axis, reflection through planes, and inversion through central point and combinations of these operations. All the symmetry operations that are related to one another by similarity transformations form a class within the group. Two elements A and B will form a class if,

$$B = X^{-1}AX$$

where *X* is an arbitrary element of the group. *A* and *B* are said to be conjugate to one another.

### 3.1 Matrix representation of a group.

All the elements of a symmetry group of a crystal can be represented by matrices which transform in the same way as the elements themselves. Thus, these matrices also form a mathematical group which forms the group representation. In two dimensions identity, n-fold rotation and reflection has the following matrix representations respectively.

$$E = \begin{pmatrix} 1 & 0 \\ 0 & 0 \end{pmatrix},\ C_n = \begin{pmatrix} \cos\frac{2\pi}{n} & \sin\frac{2\pi}{n} \\ -\sin\frac{2\pi}{n} & \cos\frac{2\pi}{n} \end{pmatrix},\ \sigma = \begin{pmatrix} -1 & 0 \\ 0 & 1 \end{pmatrix}$$

In three dimensions there are improper axis of rotation and two mirror planes. However these operations are not present in two dimensions. In three dimensions $3 \times 3$ matrices describe the operations in space. The identity, Reflection in the *xy* plane, inversion and n-fold rotation has the following matrix representations respectively.

$$E = \begin{pmatrix} 1 & 0 & 0 \\ 0 & 1 & 0 \\ 0 & 0 & 1 \end{pmatrix},\ \sigma_Z = \begin{pmatrix} 1 & 0 & 0 \\ 0 & 1 & 0 \\ 0 & 0 & -1 \end{pmatrix},\ C_n = \begin{pmatrix} \cos\frac{2\pi}{n} & \sin\frac{2\pi}{n} \\ -\sin\frac{2\pi}{n} & \cos\frac{2\pi}{n} \end{pmatrix}$$

$$i = \begin{pmatrix} -1 & 0 & 0 \\ 0 & -1 & 0 \\ 0 & 0 & -1 \end{pmatrix}$$

The sum of the diagonal elements of a matrix is called its trace or the character of the matrix.

**Table 2: Characters of the symmetry operations in three dimensions.**

| Symmetry Operation | Character $\chi$(R) |
|---|---|
| $E$ | 3 |
| $C_n$ | $2\cos\theta + 1$ |
| $\sigma$ | 1 |
| $S_n$ | $2\cos\theta - 1$ |
| $I$ | -3 |

Thus it is possible to represent the point group elements in a matrix form. But matrix representation of a point group is not unique. There may be many such matrices which transform in the same way as the symmetry operations themselves. But all such matrices can be reduced to the one single *irreducible* form also known as *irreps*. The matrices which are reducible can be represented in a block diagonal form. All the semmetry operations of a point group that belong to same class can be reprented by the same *irrep.*

 

**3.2 Symmetry and lattice vibrations**

Vibration al characteristics of the extended lattice of atoms can be described in terms of normal mode of vibration. Symmetry as applied to the crystal lattice can also be applied to the wave vectors $\boldsymbol{k}$ in the Brillouin Zone. The set of point group operations which transform the wave vector $\boldsymbol{k}$ into itself or an equivalent wave vector form the point group of the wave vector. For the zone center $\boldsymbol{k} = 0$(at the centre of the BZ), the point group of the of the real lattice is also the point group of the wave vectors.In a real crystal lattice the Bloch wave function is reprented as

$$f(\boldsymbol{R}) = \boldsymbol{U_q}(\boldsymbol{R})\, e^{i\boldsymbol{q}.\boldsymbol{R}} \tag{1}$$

Where $\boldsymbol{U_q}(\boldsymbol{R})$ is the displacement of the atom at position $\boldsymbol{R}$ from its equilibrium position for a phonon of wave vector $\boldsymbol{q}$. Let $C_n$ be transformation matrix for an n-fold rotation about a fixed axis than

$$C_n\{\boldsymbol{U_q}(\boldsymbol{R})\, e^{i\boldsymbol{q}.\boldsymbol{R}}\} = \{C_n\boldsymbol{U_q}(\boldsymbol{R})\}\boldsymbol{e}^{i\boldsymbol{q}.CR} = \boldsymbol{U}_q{}^*(\mathbf{R})\boldsymbol{e}^{i\boldsymbol{q}.\boldsymbol{R}}e^{i\boldsymbol{Q}.\boldsymbol{R}} \tag{2}$$

The character of the symmetry operation $C_n$ will be the trace of the transformation matrix multiplied by the factor $e^{i\boldsymbol{Q}.\boldsymbol{R}}$

$$\chi(\theta) = \sum_u(\pm 1 \pm 2\cos\theta)\, e^{i\boldsymbol{Q}.\boldsymbol{R}} \tag{3}$$

Where the summation in the expression (1.13) is over the unit cells.For the of the Brillouin Zone the wave vector Q=0 and thus the point group of the crystal can be used to study the vibraions in the lattice. The physical interpretation of this fact is that in lattice mode vibrations we consider the normal mode vibration of the unit cell rather than for a molecule. For experimental purpose $\lambda \approx 5000$ Å and therefore $k = \frac{2\pi}{\lambda}$ is very small compared to the B.Z dimensions and hence we consider the Γ point of the B.Z. The fundamental postulate of the crstal physics is the Neuman's Principle which allows us to corelate the symmetry of a crystal with is physical properties.

Neumann's Principle: Consider an operation of the form $E = MC$, where C is a matrix represents the physical change, $M$ is the transformation matrix and $E$ the mtrix representing the external effect (stress, electric field, etc.) .The symmetry of the physical property of a crystal must include some spatial symmetry characteristics as the crystal structure and thus the symmetry of $M$ must include all the symmetry properties contained in the point group of the crystal.

## 4. GROUP THEORETIC STUDY OF PHONONS IN THE ZNO WUTZITE STRUCTURE

The wurtzite structure of the ZnO has two inter-penetrating sub-lattices, one belonging to Zn atom and the other belonging to O atom. The wurtzite structure blongs to the spce group $C_{6v}{}^4$ where $C_{6v}$ refers to the point group of the unit cell and the superscript refers to the space group index based on its point group.Thus the unit cell is hexagonal and hence the point group of the crystal is $C_{6v}$. The Raman modes and Infrared modes can be elucidated from the character table of the point group. Character table is basically a tabulated representation of all the classes of the symmetry operations in a coloumn along with their charcters in different representations. All the symmetry operations in a class have the same character.Vibrational Raman spectra of molecules has certain selection rules. A vibrational mode of a molecule will show Raman spectra i.e. it will be Raman-active if if the polariziability of the molecules changes during the vibration. The transition integral is thus given by

$$\int_{-\infty}^{+\infty} \Psi_{\mathrm{v}}^{(\mathrm{g})}\alpha\Psi_{\mathrm{v}}^{(\mathrm{ex})}d\tau$$

Where α is the polariziablity operator of the molecule which is one of the following quadratic function function of the Cartessian coordinates: $x^2, y^2, z^2, xy, yz, zx, (x^2 - y^2)$. The function $\Psi_{\mathrm{v}}^{(\mathrm{g})}$ and $\Psi_{\mathrm{v}}^{(\mathrm{ex})}$ are the vibrational wave functions of the ground and the excited state respectively. Thus a vibration is Raman-active if it has the same *irrep* as one of the quaratic or binary cartessian coordinates listed above [8]. As discussed earlier in the representation theory, a symmetry operation may have many matrix repsentations which can be reduced to one single irreducible form in a particular dimension.The sum of the dimensions of the irreducible representationa of a group to equal to the order of the group.

$$\sum_j d_j^2 = h \tag{14}$$

Where h is the order of the group.The Reduction Formula helps in determining how many times the jth irrep is contained in a rep(reducible representation). In general any rep can be can be written as the linear combinations of the irreps. In the *Bethe notation* $\Gamma_1$, $\Gamma_2$ ....etc. are used for the irreps. In the *Mulliken notation* the irreps are represented as $A_1$, $A_2$, $E_1$, $E_2$ . Notation $A$ is used for the one-dimensional representation and $E$ for the two-dimensional representations.This notation will be used for the discussion of the Ramam-active modes.The number of times the jth irrep is contained in the reducible representation of a group of order $h$ is given by the formula:

$$n_j = \frac{1}{h}\sum_R \chi_j(R)\,\chi(R) \tag{16}$$

Where $\chi_j(R)$ is the character of the $j^{\text{th}}$ irreducible representation and $\chi(\boldsymbol{R})$ is the character of the same operation in the reducible representation. Using these group theoretical techniques it is pssible to construct the character table of the $C_{6v}$ point group of the corresponding to the hexagonal unit cell of the Wurtzite ZnO. It was allready discuused earlier that the vibrational modes corresponding to the zone-center optical phonons can be elucidated from the character table of point group of the unit cell of a lattice{Ref.eqn(1.13)}. The point symmetry group $C_{6v}$ of the wurtzite unit cell has the following elements:

$$\{E, C_6, C_6^5, C_3, C_3^2, C_2, \sigma_{v,1}, \sigma_{v,2}, \sigma_{v,3}, \sigma_{d,1}, \sigma_{d,2}, \sigma_{d,3}\}$$

 

All these twelve symmetry operations can be further classified into six classes. The symmetry operations which are linked in such a way that one operation can be transformed into the other by the operation in the group itself, belong to the same class and has the same irreducible representation. Mathematically, such elements are said to be conjugate to one another. They are related to each other by means of similarity transformation. Thus, these twelve elements are divided into the following six classes:

$$E = \{E\}$$
$$2C_6 = \{C_6, C_6^5\}$$
$$2C_3 = \{C_3, C_3^2\}$$
$$C_2 = \{C_2\}$$
$$3\sigma_v = \{\sigma_{v,1}, \sigma_{v,2}, \sigma_{v,3}\}$$
$$3\sigma_d = \{\sigma_{d,1}, \sigma_{d,2}, \sigma_{d,3}\}$$

To determine the irreducible representations of the vibrational modes at the zone center, i.e. for deducing the *irreps* of the zone center optical phonons, the following points are considered as rules:

- The point symmetry group of the unit cell is determined.
- Reducible representation of all the symmetry operations is obtained.
- Reducible representation (rep) is split into the irreps using the standard reduction formula.

As there are six classes there are six irreducible representations, since the number of *irreps* is equal to the number of classes in the group. Therefore, using equation (1.14) we have

$$\sum_{j=1}^{6} d_j^2 = 12$$

The solutions to this equation are

$$d_1 = 1, d_2 = 1, d_3 = 1, d_4 = 1, d_5 = 2, d_6 = 2$$

Thus, there are four one-dimensional representations and two two-dimensional representations.
In two dimensions the rotation operation through an angle φ is represented by the matrix:

$$R(\varphi) = \begin{pmatrix} \cos\varphi & \sin\varphi \\ -\sin\varphi & \cos\varphi \end{pmatrix}$$

The character χ(R) of this operation is

$$\chi(\mathrm{R}) = 2\cos\varphi$$

Thus, the characters of each rotational class are

$$\chi(2C_6) = \chi(\frac{\pi}{3}) = 1,$$

$$\chi(2C_3) = \chi(\frac{2}{3}\pi) = -1,$$

$$\chi(C_2) = \chi(\pi) = -2$$

The mirror reflection in two dimensions we have the operations defined as:

$$\sigma_{\mathrm{v},1} = \begin{pmatrix} -1 & 0 \\ 0 & 1 \end{pmatrix}, \sigma_{\mathrm{d},2} = \begin{pmatrix} 1 & 0 \\ 0 & -1 \end{pmatrix}$$

The characters of these operations are:

$$\chi(3\sigma_v) = 0$$
$$\chi(3\sigma_d) = 0$$

respectively. In one-dimensional *irreps* the character is either 1 or -1 depending on whether the parity of the system is conserved or not conserved in the operation respectively. For a cyclic group all entries of the character table may not be real. The $C_6$ rotation group is cyclic group of order 6. The complex character for rotation of order n is given by the $n^{th}$ root of unity

$$\in_n^m = exp(\frac{2\pi i m}{n}) = cos(\frac{2\pi m}{n}) + i\, sin(\frac{2\pi m}{n})$$

Using $n = 6$, the complex characters of the $C_6$ rotation group can be obtained. In applying group theory to physical problems, the characters need to be real and therefore the sum of the two complex roots is used for the characters of the real representation. The columns corresponding to complex rotation of order 6 can be filled by the roots of unity given by

$$\varepsilon = exp(\frac{\pi i}{3})$$

 

**Table 3: The character table of the $C_{6v}$ point group**

| $C_{6,v}$ | $E$ | $2C_6$ | $2C_3$ | $C_2$ | $3\sigma_v$ | $3\sigma_d$ | Linear Functions | Quadratic Functions |
|---|---|---|---|---|---|---|---|---|
| $A_1$ | 1 | 1 | 1 | 1 | 1 | 1 | z | $x^2+y^2$, $z^2$ |
| $A_2$ | 1 | 1 | 1 | 1 | 1 | −1 | $R_z$ | - |
| $B_1$ | 1 | −1 | 1 | −1 | 1 | −1 | - | - |
| $B_2$ | 1 | −1 | 1 | −1 | −1 | 1 | - | - |
| $E_1$ | 2 | 1 | −1 | −2 | 0 | 0 | (x, y) ($R_x$, $R_y$) | (xz, yz) |
| $E_2$ | 2 | −1 | −1 | 2 | 0 | 0 | - | ($x^2$-$y^2$, xy) |

Using the reduction formula of equation (1.16) we have,

$$\Gamma = A_1 + A_2 + B_1 + B_2 + E_1 + E_2$$

**Table 4: The character table of the $C_6$ rotational point group**

| $C_{6,v}$ | $E$ | $2C_6$ | $2C_3$ | $C_2$ | Linear Functions | Quadratic Functions |
|---|---|---|---|---|---|---|
| $A_1$ | 1 | 1 | 1 | 1 | Z, $R_Z$ | $x^2+y^2$, $z^2$ |
| $B_1$ | 1 | -1 | 1 | -1 | | |
| $E_1$ | 2 | 1 | 1 | -2 | (x, y) ($R_x$, $R_z$) | (xz, yz) |
| E2 | 2 | -1 | 1 | 2 | | ($x^2$-$y^2$, xy) |

Using the reduction formula of equation (1.16) we can find the irreducible representation of the rotational point group $C_6$. The zone center optical phonons can then be classified by the following irreducible representation

$$\Gamma = A_1 + E_1 + 2E_2 + 2B_1$$

**4.1 Raman spectrum of wurtzite ZnO**

Each primitive cell of ZnO has four atoms that lead to 12 phonon branches viz-9 optical modes and 3 acoustic modes [9]. At the center of the B. Z. (Γ-point), lattice optical phonons have the irreducible representation given by equation (1.19). In the irreducible representation $A_1$ and $E_1$ are polar modes which are both Raman and Infrared active. $E_2$ modes are non-polar modes and are only Raman active. The non-polar $E_2$ modes have two wavenumbers viz. $E_2$ (high) and $E_2$ (low) related to the motion of oxygen and zinc sub-lattice respectively. Strong $E_2$ (high) mode is a characteristic feature of wurtzite lattice. The vibrations $A_1$ and $E_1$ modes can polarize in unit cell resulting in an electrostatic field that splits the polar modes into LO and TO components. The $E_1$(LO) mode is associated with the presence of oxygen vacancies, interstitial Zn or their complexes [10]. The $B_1$ modes are Raman and infrared inactive. These are called silent modes. The number of atoms per unit cell of wurtzite ZnO is 4. The arrangement of Zn and O along the c axis is shown in figure.5.

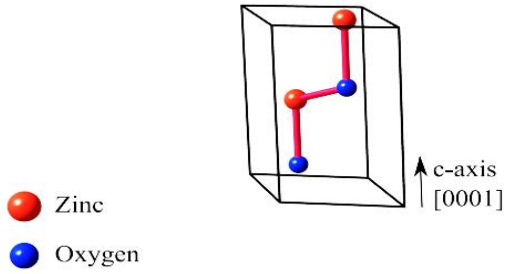


**Fig. 7: Arrangement of zinc and oxygen atom along the c-axis**

**Table 5: Acoustic and optical phonon modes in crystal with ZnO wurtzite symmetry having *S* number of atoms per unit cell**

| Mode Type | Number of modes |
|---|---|
| Longitudinal Acoustic | 1 |
| Transverse Acoustic | 2 |
| Total Acoustic Modes | 3 |
| Longitudinal Optical | $S$-1 |
| Transverse Optical | 2$S$-1 |
| All Optical Modes | 3$S$-3 |
| All Modes | 3$S$ |

Thus, in ZnO wurtzite crystal there are 12 phonon modes viz. 1longitudinal acoustic (LO), 2 transverse acoustic (TO), 3 longitudinal optical (LO) and 6 transverse optical (TO) [10]. These phonons in the wurtzite symmetry are fully characterized by the motion of the four basis atoms. Figure.6. shows the atomic displacements corresponding to the different modes of vibration in a unit cell shown in figure.5. For the A and B modes the displacements are directed along the c-axis. The A mode pattern is composed of an oscillation of the rigid Zn versus O atoms. As the Zn-O bond is polar, it results in an oscillating polarization.

 

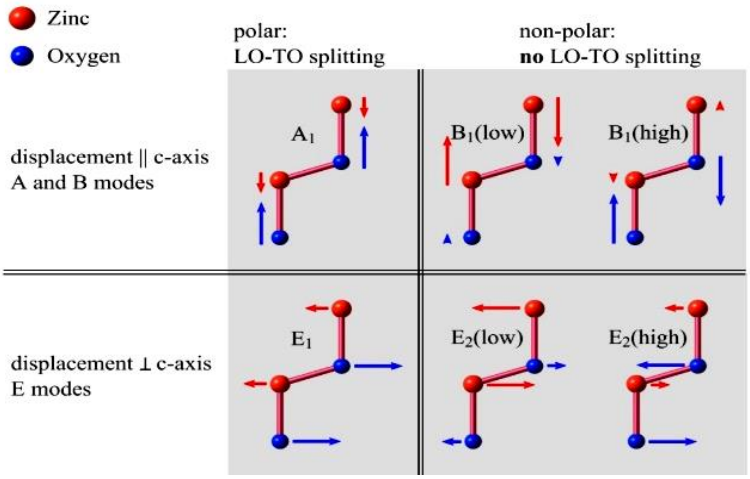


**Fig. 8: Optical phonon modes of the ZnO unit cell**

While for B modes one sub-lattice is devoid of any motion. The neighboring atoms in the other sub-lattice move in opposite direction. The $B_1$(low) mode correspond to the motion of heavier Zn sub-lattice, and the $B_1$(high) mode is associated with the motion of light O sub-lattice. Therefore, the A mode is polar and B mode is non-polar. The B mode induces no net polarization. The atomic displacements which are perpendicular to the c-axis gives rise to E mode. The oscillations of both rigid sub-lattices give the $E_1$ mode and hence the $E_1$ exhibits an oscillating polarization. The $E_2$ mode is associated to the oscillation of one sub-lattice while the other is at rest. The $E_2$ (Low) mode is essentially related to the oscillation of the Zn sub-lattice and the $E_2$ (High) mode is essentially associated with the oscillation of O sub-lattice. These are non-polar modes. A Raman spectrum of a ZnO at different temperature ranging from room temperature to 1000 $^{o}$C is shown in figure. 7. Multi-Phonon Process: Multi-phonon process can correspond to combinations, overtones and differences [11].

- One-Phonon Process: These are the fundamental processes.
- Two-Phonon Process: If both the phonon modes belong to the same irreducible representation than they are termed as overtones. However, if the two phonon modes belong to different irreducible representations, they are called combinations. There can be either addition combination or difference combination.
- Three-Phonon Process: Three-phonon process gives rise to pure combinations, pure overtones and pure mixtures.

## 5. RAMAN SPECTRUM OF THE ZnO SAMPLE AND ITS ANALYSIS.

The Raman spectrum of the ZnO sample taken for the purpose of this inquiry is given in figure 9. The room temperature frequencies corresponding to the first and second order Raman spectra is analyzed and listed in table. 6 and compared with the literature reported in Ref [12].

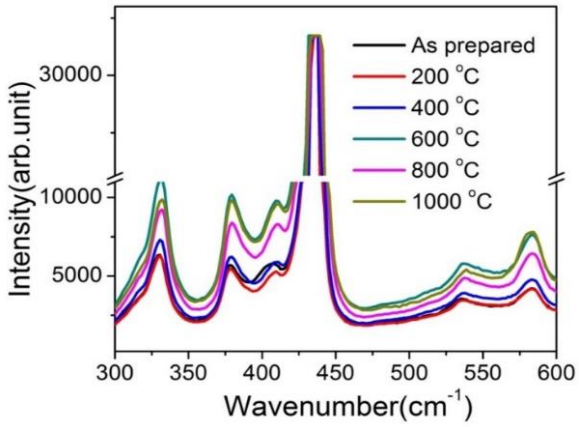


**Fig. 9: Raman spectrum of ZnO powder sample**

In figure 9. The Raman spectrum of ZnO powder sample at different temperatures is shown. The intensity is represented in arbitrary units and the frequencies in $cm^{-1}$. For the analysis of the sample the $A_1$(LO) and $E_1$(LO) modes have been considered. The intensity variations of these modes provide essential detail about the defect properties. For the present work, the analysis of the peak intensities and FWHM has been done using the analysis software named Origin. The two peaks $A_1$(LO) and $E_1$(LO) occur roughly near the frequencies 540 $cm^{-1}$ and 580 $cm^{-1}$ respectively. As is evident from the spectrum, the peak intensities for all the modes show an increase with temperature. The low frequency range up to 586 $cm^{-1}$ shows fundamental Raman modes. The frequencies 289.61 $cm^{-1}$ and 334.51 $cm^{-1}$ are the overtones. The mid frequency range above 586 $cm^{-1}$ up to 808.29 shows overtones. Since the $E_1$(LO) modes are associated with the Oxygen vacancies and Zinc interstitials, its intensity and FWHM corresponding to different temperature, ranging from room temperature to 1000 $^{o}$C, is important for studying the phonon life times. The polar $A_1$ modes which are also Raman active can reveal important information related to the phonons. The frequencies 540 $cm^{-1}$ and 580 $cm^{-1}$ corresponding to the $A_1$ and $E_1$ mode respectively at different temperature have been analyzed and the intensity and FWHM has been plotted as a function of temperature.

 

**Table 6: Room temperature frequencies of the Raman spectra of ZnO nanoparticles of the sample**

| Frequency($cm^{-1}$) | Symmetry | Process |
|---|---|---|
| 100.64 | $E_2$ | $E_2^{low}$ |
| 208.61 | $A_1$, $E_2$ | $2TA$, $2E_2^{low}$ |
| 289.61 | $A$ | $B_1^{high}$-$B_1^{low}$ |
| 334.51 | $A_1$, ($E_1$, $E_2$) | $E_2^{high}$-$E_2^{low}$ |
| 384.10 | $A_1$ | $A_1(TO)$ |
| 411.34 | $E_1$ | $E_1(TO)$ |
| 440 | $E_2$ | $E_2^{high}$ |
| 489.3 | $A_1$ | $2LA$ |
| 542.16 | $A_1$ | $A_1(LO)$ |
| 586.06 | $E_1$ | $E_1(LO)$ |
| 654.56 | $A_1$ | $LA+TO$ |
| 697.59 | $A_1$ | $LA+TO$ |
| 708.17 | $A_1$ | $LA+TO$ |
| 717.60 | $A_1$ | $LA+TO$ |
| 728 | $A_1$ | $LA+TO$ |
| 743.4 | $A_1$ | $LA+TO$ |
| 771.4 | $A_1$ | $LA+TO$ |
| 800.07 | $A_1$ | $LA+TO$ |
| 808.29 | $A_1$ | $LA+TO$ |
| 813 | $A_1$, $E_2$ | $A_1(TO)+E_2^{high}$ |
| 835.67 | $E_1$ | $2E_1(TO)$ |
| 983.84 | $E_1$ | $E_1(TO)+E_1(LO)$ |
| 1007.7 | $E_1$ | |
| 1018.81 | $E_1$, $E_2$ | $E_1(LO)+E_2$ |

## 6. RESULTS OF THE PHONON LIFETIME CALCULATION

The lifetime of phonons have been calculated from the Raman spectra. The FWHM values obtained by analysing the spectra can be used in calculating the phonon lifetime. Using the time-energy uncertainty relation

$$\frac{1}{\tau} = \frac{2\pi\Delta E}{h} = 2\pi c\Gamma$$

Where $\Delta E$ is the uncertainty in the energy of the phonon mode, h is the Planck constant and $\Gamma$ is the FWHM of the Raman peak in the units of $cm^{-1}$ [12]. From the Raman spectra various data such as the intensity, FWHM, intensity ratio, FWHM ratio for the $A_1LO$ and $E_1LO$ peaks have been extracted. These are obtained from the spectrum at different temperatures ranging from room temperatur to 1000 $^oC$. A calculation of the phonon lifetime for the $A_1LO$ and $E_1LO$ mode has been carried out. The variation of the all these readings with temperature has also been studied.

**Table 7: Phonon lifetime of the $E_1(LO)$ and $A_1(LO)$ modes of ZnO at different temperature**

| Mode | Phonon lifetime($\tau$) x $10^{-12}$s | | | | | |
|---|---|---|---|---|---|---|
| | As prepared | 200 $^oC$ | 400 $^oC$ | 600 $^oC$ | 800 $^oC$ | 1000 $^oC$ |
| $E_1(LO)$ | 0.72 | 0.68 | 0.7 | 0.704 | 0.729 | 0.78 |
| $A_1(LO)$ | 1.66 | 1.53 | 1.49 | 1.44 | 1.47 | 1.35 |

The effect of the temperature variation on the peak intensity, FWHM and their ratios are graphically represented as under.

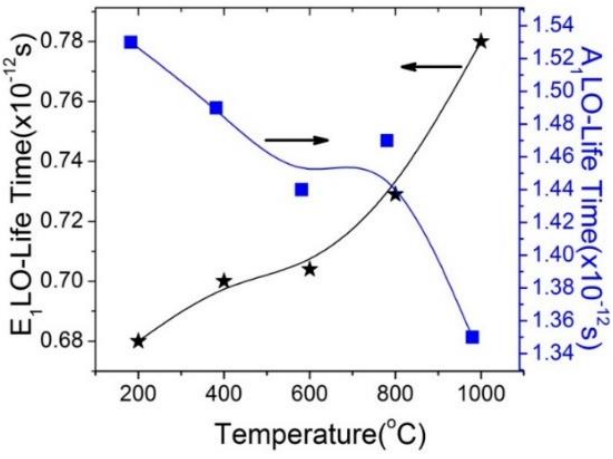


**Fig. 10: Phonon lifetime vs temperature**

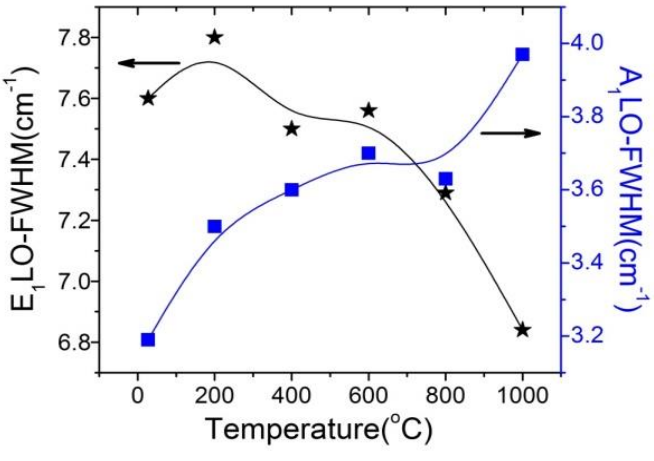


**Fig. 11: FWHM vs temperature**

 

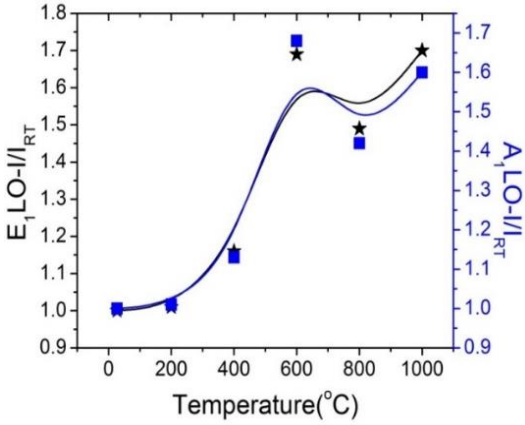


**Fig. 12: Intensity ratio vs temperature**

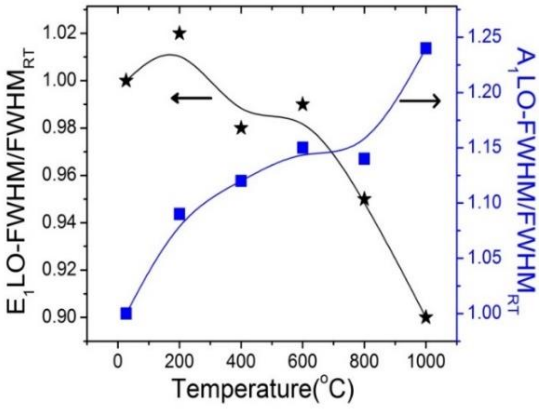


**Fig. 13: FWHM ratio vs temperature**

## 7. CONCLUSION

The phonon lifetime for the two modes shows contrasting characters. The phonon lifetime for the $A_1$(LO) mode decreases with temperature whereas the phonon lifetime for the $E_1$(LO) mode shows an increase with temperature. FWHM being inversely proportional to the phonon lifetime shows the reverse characteristics. The intensity ratio for both the modes increases with increase in temperature. The $E_1$(LO) mode is associated with the presence of the Oxygen vacancy and Zn interstitials. At high temperatures the phonon lifetime of this mode is higher than that at room temperature. Oxygen vacancy is very important for the gas sensing application of ZnO. Thus, temperature higher than the room temperature will favor the sensor functionality of ZnO sensor by enhancing the Oxygen vacancy defect.

## 8. REFERENCES

[1] J. P. Srivastava, Elements of Solid-State Physics, PHI.
[2] Mc. Euen and C. Kittel, Introduction to Solid State Physics, Wiley.
[3] G. W. Hansonm, Fundamentals of Nanoelectronics, Pearson.
[4] R. Kumar, O. AL-Dossary, G. Kumar, and A. Umar, Nano-Micro Lett. *7(2)*, 97 (2015).
[5] M. W. Ahn, K. S. Park, J. H. Heo, and S. H. Hang. Appl. Phys. Lett. *93*, 263103 (2008).
[6] P. M. A. Saherwood, Vibrational Spestroscopy of Solids, Cambridge University Press.
[7] R. C. Powell. Symmetry, Group Theory and the Physical Properties of Crystal, Sringer.
[8] R. Puri, K. Sharma, and R. Pathania. Principles of Physical Chemistry, VPC.
[9] H. Morkoc and S. Orguz. Zinc Oxide Fundamentals, Materials and Device Technology. Wiley-VCH
[10] Julius, A. Mart, L. Hardeen and P. Laous. Bulletin of Academy of Sciences, University of Urzburg (2008).
[11] H. W. Kunnert, D. J. Brink, F. D. Auret, J. Malherbe, J. Barnas, and V. Kononenko. Phys. stat. sol (c) 2, 1131 (2005)
[12] R. Cusco, J. Jimenez, B. Wang, and M. J. Callahan. Phys. Rev. B 75, 165202 (2007)
[13] N. Han, X. Wu, L. Chai, H. Liu, and Y. Chan. Sens. Actuat. B: Chem. *150*, 70 (2010).
[14] J. Huang, Q. Wan, L. Wang, and T. L. Hans. Sensors *9*, 9903 (2009).
[15] M. W. Ahn, K. S. Park, J. H. Heo, and S. H. Hang. Appl. Phys. Lett. *93*, 263103 (2008)
[16] D. K. Diao, M. Zhou, J. Zhang, Y. Tang, and S. Wang. Sens. Actuat. B Chem. *219*, 30 (2015).
[17] S. M. Chou, L. G. Teoh, W. H. Su, and M. H. Hon. Sensors. *6*, 1420 (2006).
[18] Y. F. Sun, S. B. Liu, F. L. Meng, J. Y. Liu, Z. Jin, and L. T. Kuong. Sensors, *12*, 2610 (2012).
[19] C. N. Xu, J. Tamaki, N. Miura, and N. Yamazoe. Sens. Actuat. B *3*, 147 (1991).
[20] P. Mitra and A. K. Mukhopadhayay, Bull. Pol. Acad. Sci., Tech. Sci. *55*, 203 (2006).

 